https://doi.org/10.2352/ISSN.2169-4451.2017.32.348

Meniscus Motion Inside A DoD Inkjet Print-Head Nozzle

Claudio S Ravasio, Wolfson College Cambridge, UK; Stephen D Hoath and Graham D Martin; University of Cambridge, Cambridge, UK; Peter Boltryk and Marko Dorrestijn, Xaar, Cambridge, UK

Abstract

A new study of the jetting performance for drop-on-demand (DoD) inkjet print heads investigated meniscus motions inside the transparent nozzles of MicroFab inkjet print heads. A composite image representation of the observed meniscus motions, imaged at high resolution using a spark flash light source, was developed for our subsequent analyses of the influences of drive voltage and pulse dwell time and also the ink properties. At higher drive voltages a slow damped refill (following de-pinning of the meniscus from the very edge of the nozzle exit) was also clearly observed. This and many other interesting phenomena were observed with the composite images: internal bubbles that progressed through the nozzle region over relatively long timescales, internal break-off of the jet from the meniscus surface, satellite formation and merging, and the contact line de-pinning not previously observed before..

Introduction

Industrial inkjets operate at high line-printing frequencies to help improve productivity and to access new applications. Precision delivery of liquid drops is achieved at low frequencies but gets limited at higher frequencies by the variations in initial meniscus conditions from drop to drop. This study of jetting from a transparent MicroFab nozzle complements research work on Xaar inkjet print-heads.

Inkjet drive voltage determines the jetted drop speed and drop volume ejected from piezoelectric DoD inkjet print-heads. Fluid properties affect the relative importance of inertia, viscosity and surface tension in determining this response. Raising the piezoelectric drive voltage at a given printing frequency not only increases the jetted drop speed and volume but also the residual amplitudes of the ink meniscus motions, persisting well beyond the duration of the waveform [1-4].

Experimental

A conventional microscope-based automatic jetting rig captured back-lit images using a 20ns spark-flash source triggered at fixed delay intervals increasing by 1 or 2µs delay steps up to 2000µs after the print-head drive trigger. Image sequences of successive jet triggering events were then processed using MATLAB to extract the meniscus behavior. Figure 1 shows an annotated horizontal image view of a nozzle.

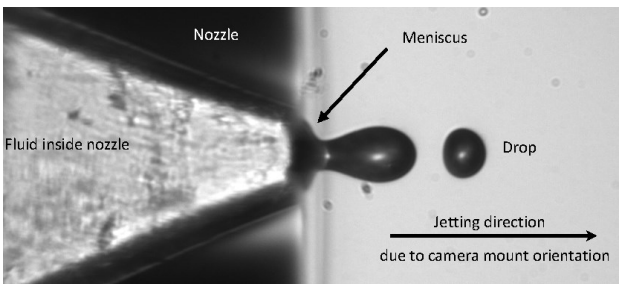

Figure 1*. An annotated image of the drop ejection process*

Image analysis method

For each measurement, the data were generated as a series of 200-2000 images. For tracking the meniscus and drop movements in large numbers of images, a new method of representing the data was implemented. The method essentially consists of combining the center line through the nozzle from each image in the same series. The composite images created that way show meniscus and drop movements at a glance.

The method was implemented in MATLAB, making use of the Image Processing Toolbox. The composite images were analysed based on pixel brightness (greyscale level); Figures 2 and 3 are annotated to highlight key features that were reliably seen. The reliable interpretation of composite images was supplemented by using the raw shadowgraph data in video form. The latter included de-pinning, which will be shown at NIP32.

From the sequential images with fixed delay increments, sequences of flash images of jetting events were automatically processed by extracting a typical line along the symmetry axis of the jetting event within each image, as shown in Figure 2, then stacking successive event "lines" along (downwards) time axis to create a composite image which displays the historical progression of the meniscus position and jet tip, as shown for example in Figure 3. Some further technical adjustments were automated in the MATLAB code to locate the symmetry axis and partially compensate for the flash image background intensity variations occurring from image to image.

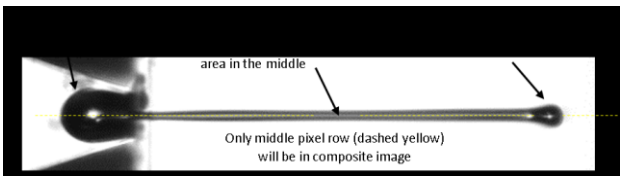

Figure 2. Reduction of a shadowgraph image of a transparent jetting nozzle to a single line, highlighting key features that were reliably seen.

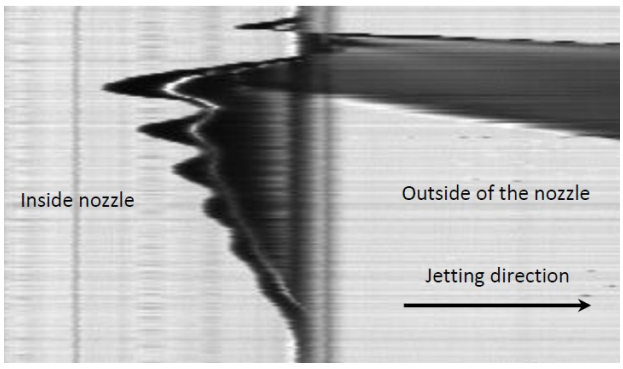

Figure 3. Elapsed time progresses vertically downwards in the composite image; the transparent nozzle exit is a thin vertical black line; while the light region to the left is ink inside (due to the similar refractive index to the glass nozzle), it is dark where air is inside the nozzle; jetted ink to the right appears darker than air (as usual in such shadowgraphs).

Inspection of Figures 2 and 3 shows the method does clearly track the positions of several features inside and outside the nozzle. Inside the nozzle, the initial (fast) retraction of the ink meniscus is quickly followed by the emergence of the inkjet outside the nozzle at a rate determined by the jet tip speed. After emergence, but before the inkjet ligament finally separates from the meniscus, there may be some delay before the meniscus retracts into the nozzle. In Figures 2 and 3, the break-off occurs within the glass nozzle but before the maximum retraction of the meniscus is reached. After the jetting event the meniscus exhibits some oscillations and a gradual recovery towards the nozzle exit. Extra details, such as bright spots appearing due to the optical lens action of the hollow tapered glass nozzle when the meniscus is retracted within the nozzle and also from the near-spherical optics formed by the transparent ink in the jet head, can also be tracked as secondary information about the motion of ink both inside and outside the print-head.

Figure 4 shows a similar sequence annotated with some of these key features of the inkjet and meniscus motion, together with notes on the characteristics that can be gleaned from these quantitative observations.

The following features of the composite images were initially used to create parameters for our interpretation of the measurements: 1) z_0, the maximum retraction of the meniscus after a jetting event; 2) t_r, the elapsed time taken for the meniscus to first reach the mid-line (nozzle plane); 3) v_{jet}, the initial fluid ejection speed of the jet. The first two of these empirical parameters were later combined to form another "speed": we have taken the ratio of maximum retraction to the elapsed time to recover to the mid-line position to represent a "pseudo" refill speed for our discussion purposes.

Other phenomena, as well as the characteristic parameters, are labelled in Figure 4: A) an underdamped slow recovery of the meniscus position to the nozzle plane; B) a small damped oscillation superposed on this recovering meniscus position; C) the decelerating jet tip resulting from the (surface tension) forces between it and the meniscus from the attached ligament; D) the trailing ligament pulled by the head of the ejected jet detaches from the inward- moving meniscus at the X; and E) formation of a satellite droplet with lower speed than the leading drop, implying that they will never reunite (in-flight). [5]

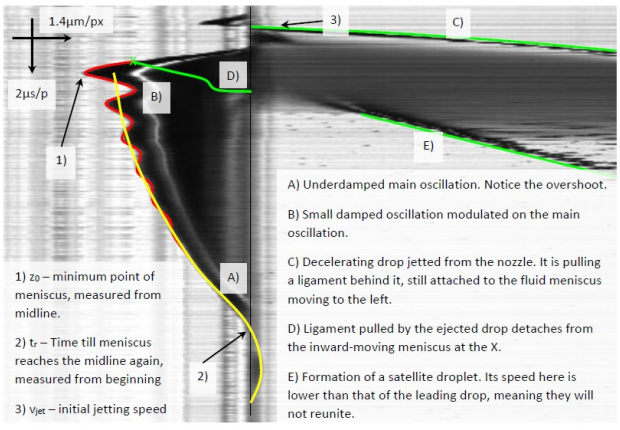

Figure 4. *A composite image [5] with superposed colored lines to guide the eye. A thin vertical black mid-line marks the nozzle exit location, showed ink had protruded beyond the nozzle plane after recovery. This data series was for jetting fluid v12-23 (see Table 1) from a 40µm diameter MicroFab nozzle with drive voltage 55V and dwell time of 16µs (defined as in Figure 5).*

The third empirical parameter, the initial fluid ejection speed for the jet, was extracted from the fitted slope of the jet tip location vs. elapsed time using Equations (1) and (2) [6]:

$$\text{Tip position } s = v_{drop}t + (v_{jet}-v_{drop})t_0\,[1-\exp(-t/t_0)] - \tfrac{1}{2}at^2 \quad (1)$$

$$\text{Tip speed } u = v_{drop} + (v_{jet}-v_{drop})\exp(-t/t_0) - at \quad (2)$$

Equations (1) and (2) represent position and speed of the jet tip after the time t following emergence from the nozzle at initial speed v_{jet} and final speed v_{drop}, including the 'small' constant deceleration term a and the 'larger' effects of inkjet ligament slowing of the jet tip via an exponential decay with timescale t_0 for attaining the final drop speed achieved after break-off. Unpublished computations, based on a simple model of DoD inkjet printing of dilute polymer solutions [7], and also our data in this study, showed this empirical representation [6] to be surprisingly accurate. Although the deceleration of inkjets and drops greatly exceeds gravity (acting oppositely, to accelerate jetted fluid) [5], it has almost no effect on the timescale relevant to these meniscus studies. In the region closest to the nozzle, the jet tip speed u always exceeded the final drop speed v_{drop} and the fitted value for the initial speed v_{jet} is only approximate.

Jetted fluid and MicroFab drive parameters

Viscosity and surface tension effects were explored using different water-glycerol and isopropyl alcohol jets to represent the extremes of high (14mPas) and low (~ 2mPas) viscosity and high (~ 40mN/m) and low surface tension (~ 20mN/m) fluids. These values span the majority of inkjet fluid properties (with the notable exception of water-based inks without additives), deliberately chosen to help elucidate meniscus motion effects.

A labelled set of fully transparent fluids were used, having the viscosity and surface tension values tabulated in Table 1. Label v12- indicates 12cP water-glycerol mix with NN% IPA, while v100 refers to pure IPA having standard viscosity (2cP).

Table 1

Test fluid label	Viscosity (mPas)	Surface Tension (mN/m)
v12-10	13.9	37.0
v12-23	14.1	28.9
v100	(2.0)	21.6

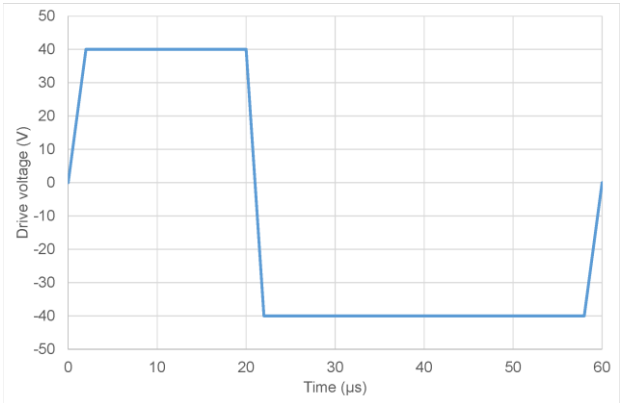

Figure 5*. An example of the MicroFab MJ-ABP print-head drive waveform used in these studies. The positive and negative voltage amplitudes were equal and opposite. The rise and fall times were 2µs irrespective of drive voltage amplitude and the duration of the "positive" dwell time (here 18µs) was always half that of the duration of the negative dwell time (here 36µs).*

A range of MicroFab nozzle diameter sizes and drive waveform duration and amplitudes were also employed to help us study the influence of these jetted fluids and (MicroFab) DoD print-head parameters on the observed characteristics and behavior of meniscus motion inside (+outside) nozzles. A fixed "meniscus pressure" retained ink against long-term dripping [8]. Nozzles of 20, 30, 40 and 50µm diameter were available, although the study only used 30-50µm nozzles (see Appendix).

Jetting from the print-head and data taking was initiated by an automatic (LABVIEW) program that appropriately triggered a MicroFab Jet Drive III controller that provided a bipolar drive voltage waveform with a preset amplitude and pulse duration, and drive voltage amplitude and pulse duration were varied to explore their effects on the meniscus behavior, in a similar way to the (semi-) empirical (or simulated [4]) optimization of jetting from industrial inkjet print-heads.

The positive voltage dwell time of the jetting waveform used was varied in steps between 12µs and 23µs, see Figure 5. For the inks used in these experiments, jetting required drive voltages above 10V; voltages were raised to 80V in steps of 5V; unstable jetting was often observed at drive voltages above 80V.

Graphical comparisons

Figure 6 exemplifies the power of the composite images by providing an immediate visual comparison method for the meniscus behavior resulting from changing a jetting parameter, here the dwell time. Despite the overfilling of the nozzle after the recovery to the mid-line for a dwell time of 14µs, meniscus motion is fully completed before even the recovery time for any of the 3 other dwell time choices (16-20µs). The small retraction peaks at the top of each series reflect the common drive voltage and fluid used, while the longer dwell time series appear to suffer from an additional high frequency component and far slower recovery to the mid-line without an overshoot.

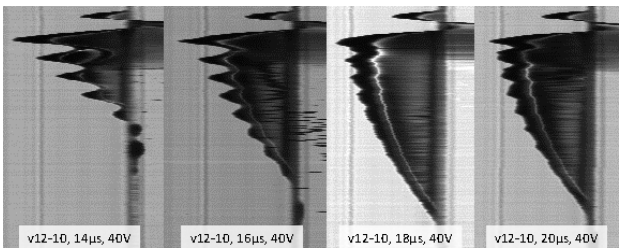

Figure 6. *Composite images of meniscus motions following a jet of the same fluid (v12-10) and drive voltage (40V) for 4 different dwell times.*

Results

The maximum meniscus retraction into the nozzle for each series (equivalent to the z_0 of Figure 4) was almost linearly dependent on the amplitude of the applied drive voltage (above a fixed threshold voltage). All values of z_0 at a specific drive voltage were, with a few exceptions, within about 5% of each other. The estimated accuracy in the value of z_0 was ±2px ≈ ±3µm. There was no clear correlation with the dwell time (12-20µs), while the fluids assessed did not seem to play a factor in the extremal retraction.

Refill time (t_r) was heavily dependent on the drive voltage value and tended to increase exponentially with this drive. The v12-23 18µs data series was the outlier, probably affected by a partial nozzle blockage. Generally, fluids with both higher surface tension and viscosity had shorter refill time. The relevance of the waveform dwell time to nozzle refill time was more difficult to assess as there was no clear trend discerned.

Discussion

The ratio z_0/t_r gives the "pseudo" refill speed v_r, which doesn't correspond to an instantaneous but an average physical speed of the meniscus, i.e. an overall measure of how quickly the nozzle refills. For jetted v12-10 it followed a right-skewed distribution as a function of the drive voltage and the pseudo refill speed tended to be faster for shorter dwell times; the peak in this ratio was found between 15V and 30V irrespective of the waveform dwell time and the refill speeds tended towards the same slow speed at the higher drive voltage used, as shown in Figure 7 within an accuracy estimated to be ±4% of speed.

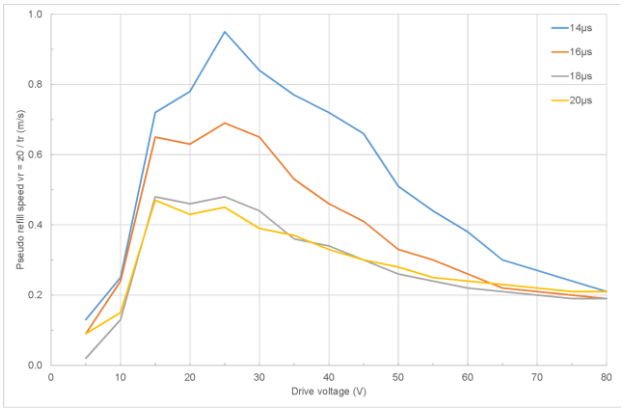

Figure 7*. Pseudo refill speed $v_r = z_0 / t_r$ as a function of drive voltage (in 5V steps) for jetted fluid v12-10 at 4 different waveform dwell times (as described in text). The uncertainties in this speed are estimated as ±4%.*

The form of this graph suggest there may be more than one mode of nozzle refill acting, with a balance related to the drive amplitude used for fluid and print-head combinations. Further work on this is clearly of interest and continues at Cambridge.

Figure 8 shows, for pre-selected drive pulse dwell times, the period of the small oscillations seen in the meniscus motions inside 40µm print head following the jetting of v12-10 and v12-23 inks at drive voltages similar to, or well above, the voltages of peaks in the "pseudo" refill speed seen in Figure 7. Apart from the v12-23 18µs data series, which also appears to be anomalous in other plots of variables (not shown), these inks had rather different sensitivity to the dwell time. The v12-23 series data had a long period which systematically (apart from 18µs) increases with dwell time, but v12-10 series data had a short period apparently uncorrelated with dwell time; all series tend towards shorter periods as the drive voltage was increased.

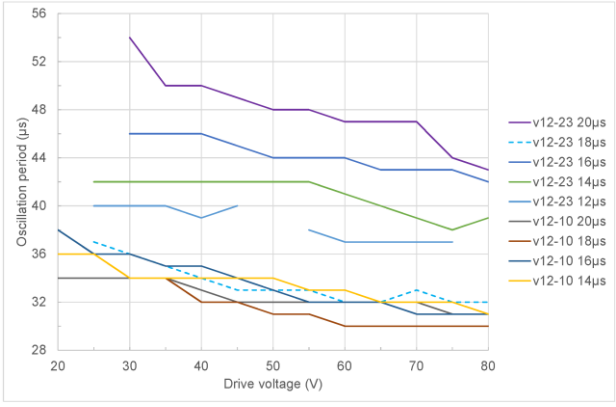

Figure 8*. Period of the small oscillations seen in the meniscus motions within a 40µm diameter MicroFab nozzle for jetted v12-10 and v12-23 inks.*

The small oscillations shown in Figure 8 arise from wave behavior. An electrical test performed on a nozzle containing the ink gave an oscillation frequency of about 34kHz, in good agreement with the COMSOL model calculations [9], and consistent with a wave period of 30μs. This value happens to correspond with the observed asymptotic limit of the period at high drive voltage, irrespective of pulse duration, for v12-10 ink.

The accuracy of the small oscillation period values in Figure 8 was estimated as ±1μs (<3%) so that these trends look real. As the two inks jetted had comparable viscosity, but differed in their surface tension by a reduction of about 20% due to the additional IPA content, we might attempt to ascribe the >+30% differences in the period of the small oscillation in the meniscus motion to this cause. However most oscillatory behaviour driven by surface tension σ has a period ~1/√(σ) [4], which implies a +10% effect that would be insufficient to account for the observations in Figure 8 of the present work.

Comments can be made about the absolute frequency values for the small oscillations: the 30, 40 or 50μs periods seen in the 40μm MicroFab nozzle diameter data series correspond to 33, 25 or 20kHz waves in the fluid, respectively. The applied waveform edges were relatively sharp, almost step-like at 2μs, corresponding to 500kHz excitation. The positive dwell times of 12-20μs correspond to repeat frequencies of 80-50kHz, again somewhat higher than 33-20kHz waves on the meniscus. As negative dwell times are double the positive dwell times they correspond to repeat frequencies of only 40-25kHz, which is the same ball-park as the observed meniscus motions and also close to the typical operation point to help suppress residual waves within piezoelectric DoD print heads [4, 10].

Initial jetting speed v_{jet} was also extracted for all fluids jetted from a 40μm nozzle using the stacked images, but the speed determined had likely inaccuracies >10%. It was found that v_{jet} increased very rapidly from 0 to reach speeds of 10-15m/s for v12-10 and v12-23 fluids and then far less rapidly (if at all) above drive voltages of 20-30V. While the trend was not very pronounced, v_{jet} was lowered by using higher dwell times. At the higher jet speeds other physical mechanisms may have limited the achievable jet speed with increasing drive, but these lie beyond the explicit purpose of the present study.

Conclusions

The meniscus visualization method developed for this study combined the benefits of graphing and imaging in a very effective manner showing both short term and longer term fluid phenomena during the jetting process. The meniscus motions observed do correspond to the usual residual oscillations within the fluid being jetted, and additional effects as the meniscus de-pinned from the nozzle exit in jetting at raised drive voltages. These changes impact the upper limit to printing frequency achievable for reliable DoD jetting, and should inform studies of industrial print-head designs. This UROP study helped Xaar via a cost-effective exploitation of University inkjet research.

Appendix: MicroFab jetting simulations

The typical internal shape and actuator geometry of the 40μm diameter MicroFab inkjet print-head nozzle used in this study were assessed by micro-sectioning similar devices. Geometrical representations of inner radial profile along the negative z-axis of the nozzle used the mathematical form [6]

$$Radius(z) = \tfrac{1}{2}\{R_2+R_1 - (R_2-R_1)\tanh((z-z_c)/z_s)\} \quad (3)$$

The volume contained between planes at z (<0) and (z=0) is

$$Volume(z) = \int \pi Radius(z)^2 dz \text{ (from } z \text{ to 0)} \quad (4)$$

Exact computation of the included volume shows that this is almost linear in z (and well-modelled by a quadratic in z) over the observed range of meniscus position. Experimental values for the nozzle profiles measured for different diameter MicroFab MJ-ABP print heads revealed our 20 μm diameter print-head profile did not correspond particularly well to the scaled 40 μm diameter profile, whereas that for a 30 μm diameter print-head profile was quite similar. The glass drawing and grinding back procedures were probably similar for these MicroFab MJ-ABP print heads, so we surmised that the external diameters of the pre-drawn glass tubes may vary slightly across nozzle diameter ranges/batches. Most of our data were taken with 40μm nozzles.

The electrical response of the piezoelectric inkjet print-head was also measured at Xaar to provide further input to (COMSOL) numerical simulations of MicroFab print-head jetting. Further details of analyses and videos are elsewhere [9].

Acknowledgements

We thank Paul Drury, Mario Massucci and Tim Wickens (Xaar Ltd), Ching Chen and Ian Hutchings (University of Cambridge Inkjet Research Centre), for support, helpful comments and the ink property measurements used for this project. This research was performed by CSR under the Undergraduate Research Opportunities Program (UROP) scheme, within the University of Cambridge Inkjet Research Centre, funded by Xaar Ltd. SDH supervised and held an EPSRC Impact Acceleration Knowledge Transfer Fellowship (grant no. EP/K5037574/1) for working with a Xaar R&D team during the initial part of this project.

References

[1] H. Wijshoff, "The dynamics of the piezo inkjet print-head operation". Phys. Rep. 491, 77-177 (2010).

[2] W.-K. Hsiao, S.D. Hoath, G.D. Martin, and I.M. Hutchings, "Jetting, In-Nozzle Meniscus Motion and Nozzle-Plate Flooding in an Industrial Drop-on-Demand Print Head". IS&T's NIP 27 66-69 (2011).

[3] J.R. Castrejón-Pita, S.D. Hoath, A.A. Castrejón-Pita, N.F Morrison, W.-K. Hsiao, and I.M Hutchings, "Time-resolved particle image velocimetry within the nozzle of a drop-on-demand print-head". J. Imaging Sci. and Technology, 56, 50401 (2012).

[4] N. Morita, A.A. Khalate, A.M. van Buul, and H. Wijshoff, in Fundamentals of Inkjet Printing: The Science of Inkjet and Droplets, S.D. Hoath (Ed), Wiley-VCH, Weinheim (2016). Chapter 3 Inkjet Print-heads.

[5] C.S. Ravasio, S.D. Hoath, M. Dorrestijn, P. Boltryk, and G.D. Martin, "Meniscus motion inside an inkjet print-head nozzle", A0 poster presented at the IOP meeting on Science of Inkjet and Printed Drops, London, UK, Nov 10th (2015).

[6] S.D. Hoath, W.-K. Hsiao, S. Jung, G.D. Martin, I.M Hutchings, N.F. Morrison, and O.G. Harlen, "Drop speeds from drop-on-demand inkjet print-heads", J. Imaging Sci. Technol. 57, 010503 (2013).

[7] S.D. Hoath, O.G. Harlen and I.M Hutchings, "Jetting behaviour of polymer solutions in drop-on-demand inkjet printing", J. Rheol. 56, 1109-1127 (2012).

[8] E.R. Lee, Microdrop Generation, CRC Press, Boca Raton FL (2003). Chapter 5 Section 5.4 Internal Pressure Level

[9] P. Boltryk, M. Dorrestijn and S.D. Hoath, unpublished (2015).

[10] J.F. Dijksman and A. Pierik, in Inkjet Technology for Digital Fabrication, I.M. Hutchings and G.D. Martin (Eds), John Wiley (2013). Chapter 3 Dynamics of Piezoelectric Print-Heads.

Author Biography

Claudio Ravasio of Wolfson College is starting his M.Eng year after a First Class degree in the Department of Engineering at the University of Cambridge, UK (2016). He holds a BSc in Environmental Engineering from ETH Zurich, Switzerland (2012). The present work was part of a summer project for Xaar at the Inkjet Research Centre in the IfM (Institute for Manufacturing), University of Cambridge, UK.